Reliability and Fairness for UAV Communication Based on Non-Orthogonal Multiple Access

Van-Lan Dao, Hung Tran, Svetlana Girs, Elisabeth Uhlemann
School of Innovation, Design and Engineering, Mälardalen University, Västerås, Sweden
{*van.lan.dao, tran.hung, svetlana.girs, elisabeth.uhlemann*}*@mdh.se*

***Abstract*—Recently, communication using unmanned aerial vehicles (UAVs) as relay nodes has been considered beneficial for a number of applications. Moreover, non-orthogonal multiple access (NOMA) with users being assigned different signal power levels while sharing the same time-frequency domain has been found effective to enhance spectrum utilization and provide predictable access to the channel. Thus, in this paper we consider an UAV communication system with NOMA and propose a solution to find the optimal values for the user's power allocation coefficients (PACs) needed to achieve the required levels of communication reliability. We present a closed-form expression for the PAC of each user and also propose an algorithm for finding the optimal altitude of the UAV required to satisfy the fairness condition for all users. Finally, we provide numerical examples and compare the results for three types of communication environments.**

I. Introduction

Recently, communication supported by unmanned aerial vehicles (UAVs) has been considered as a promising solution in both civil and military applications where UAVs can provide relay opportunities in UAV assisted ad hoc networks or act as flying base stations to serve ground users in disaster areas, battle fields, traffic congestions, sport events, agriculture, and so on [1], [2]. A UAV can cover a large area due to its rich line-of-sight to the ground users, which enables more efficient and reliable wireless communication [3], [4].

In order to increase the number of users which can be served by a UAV and enable instantaneous channel access, sharing of the communication bandwidth is required. One way to make this possible is due to recent advances of non-orthogonal multiple access (NOMA) techniques [5], where multiple users are able to share the same bandwidth and enhance their throughput by utilizing the power domain. Moreover, NOMA also provides predictable channel access delays, which is crucial for applications with strict timing and reliability requirements. A number of recent studies investigate the use of NOMA to enhance the performance of UAV based communication [6]–[10]. More specifically, in [6], Sharma *et al.* considered a system in which the UAV communicates with two ground users using NOMA. The outage probability has been derived to examine the performance of the system compared to orthogonal multiple access (OMA). In [7], a UAV system employing NOMA technique has been studied with the goal of optimizing the power allocation policy and the UAV's altitude to maximize the sum-rate for two users. However, the authors did not consider the effect that the UAV's height and the power allocation coefficient (PAC) for each user have on fairness among users and communication reliability. In [8], the authors proposed a method to find the optimal height of the UAV such that the transmitted power of the UAV is minimized while the coverage region is maximized. Similar to [7], the constrains on communication reliability and fairness among users were not taken into account, while they are crucial for, e.g., industrial applications where information should be reliably and timely delivered to all users. In [9], the authors studied the impact of relay placement on the system performance and showed that the altitude of the UAV significantly affects, e.g., power consumption and reliability.

In this work, we consider fairness among users and study UAV-based NOMA communication where the UAV must adjust its parameters to make sure that the served users are treated fair, such that reliable communication is provided. We formulate a closed-form expression to calculate the optimal power allocation for each user and propose an algorithm for finding the UAV's height and the PAC for each user that satisfy the fairness and reliability requirements set by the application. The performance of the proposed algorithm is studied in urban, sub-urban, and dense-urban environments to evaluate the effect the environmental conditions on the calculated optimum values.

The rest of this paper is organized as follows: Section II introduces the NOMA concept, Section III presents the considered channel model and communication protocol, while Section IV describes the proposed optimization algorithm. Numerical results are discussed in Section V, and Section VI provides conclusions and directions for future work.

II. NOMA Concept

Resources for traditional wireless communication are typically allocated in the time, frequency, or code domain, which led to the development of various OMA schemes such as orthogonal frequency-division multiple access (OFDM), or time division multiple access (TDMA). The major drawbacks of these methods are that they are not able to support a large number of simultaneous connections and that they require a centralized network. In order to overcome these drawbacks and provide predictable and reliable channel access to many simultaneous users, NOMA has been proposed as a promising solution [11], [12]. With NOMA, multiple

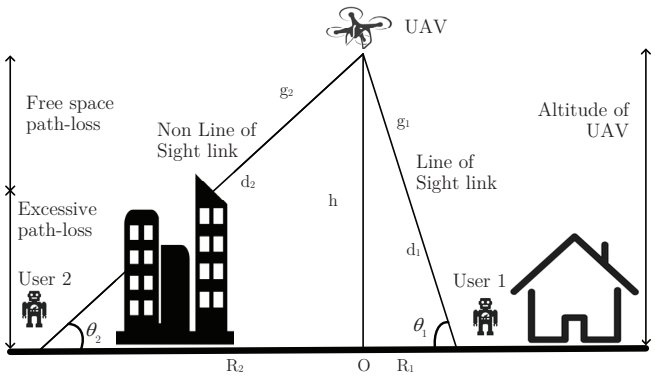

Figure 1. System model.

users share the same time-frequency resource and by having significant differences in power levels of the signals aimed towards different users, it is possible to isolate each signal even when they have been sent simultaneously. For example, let us consider the scenario shown in Fig. 1. Here, we look at an autonomous garbage collection application with one UAV is communicating with two autonomous robots (U_1, U_2). The UAV helps the robots to find the rubbish bins and also avoid obstacles to ensure safety. Without loss of generality, we assume that U_2 is located further from the UAV than U_1. In this case, U_1 requires smaller power of the signal compared to U_2. The superimposed transmitted signal from UAV to the users U_1 and U_2 is formulated as [13]

$$x = \sqrt{\mu_1 P_{\text{TX}}} x_1 + \sqrt{\mu_2 P_{\text{TX}}} x_2, \tag{1}$$

where P_{TX}, μ_i, and x_i are the transmitted power of the UAV, PAC for user U_i ($\mu_1+\mu_2 = 1$), and signal of U_i, respectively. Accordingly, the received signal at U_i can be given as

$$y_i = g_i x + n_0, \tag{2}$$

where n_0 and g_i are the additive white Gaussian noise and channel coefficient, respectively.

III. Channel Model And Communication Protocol

We consider the scenario in Fig. 1. The UAV is expected to send different control packets to different users at the same time to not only synchronize operations of the users, but also save time and enhance spectrum utilization. The UAV is located above the users at the height h, and the vertical projection of the UAV on the ground is the O point. Symbols d_i, R_i, θ_i, $i \in \{1, 2\}$ denote the distance between the UAV and the user U_i, the distance between the projection point O and the user U_i, and the elevation angle between U_i and the UAV, respectively. In this case, d_i and θ_i are calculated as follows:

$$d_i = \sqrt{R_i^2 + h^2}, \tag{3}$$

$$\theta_i = \arctan\left(\frac{h}{R_i}\right). \tag{4}$$

A. Channel model

In [14], the authors considered channel models associated with two independent groups, including users having a line of sight (LoS) or near LoS condition, and users with no line of sight (NLoS). In this paper, we use the channel model from [8], [14]–[16], i.e., the link between the users and the UAV can be considered as either LoS or strong NLoS. The probability of occurrence for each group depends on the environment profile that is defined by the altitude the density of the buildings, and the elevation angle between the UAV and the users. At the same time, the probability of having either a strong NLoS or LoS link is much higher compared to the probability of the occurrence of multi-path fading, and thus, the effect of small-scale fading can be neglected in this case [14], [16]. Consequently, the probability of LoS for each user is formulated as [8]

$$P_i(\text{LoS}) = \frac{1}{1 + \alpha e^{-\beta\left(\frac{180}{\pi}\theta_i - \alpha\right)}}, \tag{5}$$

where α and β are constants describing the environmental profile of the coverage area, e.g., urban, sub-urban, or dense urban. Also the probability of the user experiencing a NLoS link can be expressed as

$$P_i(\text{NLoS}) = 1 - P_i(\text{LoS}). \tag{6}$$

Taking the first differentiation of $P_i(\text{LoS})$ with respect to θ_i, we have

$$\frac{dP_i(\text{LoS})}{d\theta_i} = \frac{180\alpha\beta e^{-\beta\left(\frac{180}{\pi}\theta_i - \alpha\right)}}{\pi\left(1 + \alpha e^{-\beta\left(\frac{180}{\pi}\theta_i - \alpha\right)}\right)^2} > 0, \forall\theta_i. \tag{7}$$

Clearly, $P_i(\text{LoS})$ is an increasing function of the elevation angle θ_i. This means that increasing altitude of the UAV leads to an increasing elevation angle between U_i and the UAV, in which case the ground user has a better LoS link. Excessive losses are caused by reflection of the transmitted signals and shadowing due to presence of objects obstructing the paths in the coverage area. Thus, a combination of free space propagation loss and different excessive path loss is considered for strong NLoS and LoS [8]. Further, we can express the average path loss between the UAV and *i*-th user on the ground as [8]

$$L_i = \begin{cases} 20\log_{10}\left(\frac{4\pi f_c}{c} d_i\right) + \xi_{\text{LoS}} & \text{LoS link} \\ 20\log_{10}\left(\frac{4\pi f_c}{c} d_i\right) + \xi_{\text{NLoS}} & \text{NLoS link} \end{cases}, \tag{8}$$

where c, f_c are the speed of light and the carrier frequency, respectively; ξ_{LoS} and ξ_{NLoS} are the average additional losses to the free space propagation loss which depend on the environment. According to [8], the mean path loss considering the probabilities for LoS and NLoS can be formulated as

$$\overline{L}_i(R_i, h) = P_i(\text{LoS}) L_i(\text{LoS}) + P_i(\text{NLoS}) L_i(\text{NLoS}). \tag{9}$$

Substituting (6) into (9), we can rewrite $\overline{L}_i(R_i, h)$ as

$$\begin{aligned}\overline{L}_i(R_i, h) =& P_i(\text{LoS})\{L_i(\text{LoS}) - L_i(\text{NLoS})\} \\ &+ L_i(\text{NLoS}).\end{aligned} \tag{10}$$

When considering the channel model between users and the UAV that is based on probabilistic LoS and NLoS links instead of the fading channel [16], the channel coefficient between the UAV and *i*-th user on the ground can be expressed as [17]

$$g_i = \frac{1}{\sqrt{1 + \overline{L}_i(R_i, h)}}. \tag{11}$$

B. Communication protocol

We look at a scenario where the UAV transmits two packets with different information to users U_1 and U_2; and both packets should be delivered to the users before their corresponding deadlines. If a packet has not arrived before t_{out}, it is considered lost. T_i denotes the time to transmit a packet from the UAV to user U_i [18]–[21]. It can be formulated as

$$T_i = \frac{L}{W \log_2(1 + \gamma_i)} = \frac{\overline{B}}{\ln(1 + \gamma_i)}, \tag{12}$$

where $\overline{B} = \frac{\ln(2)L}{W}$, W is the system bandwidth, L is the length of the packet, and γ_1, γ_2 are signal-to-noise ratio (SNR) at U_1, signal-to-interference-plus-noise ratio (SINR) at U_2, respectively.

In NOMA, U_2 can decode x_2 directly by considering U_1's signal as interference, while U_1 gets x_1 by canceling x_2 using successive interference cancellation (SIC). Therefore, the SNR at U_1 and SINR at U_2 are obtained as

$$\gamma_1 = \frac{\mu_1 P_{\text{TX}} |g_1|^2}{N_0}, \tag{13}$$

$$\gamma_2 = \frac{\mu_2 P_{\text{TX}} |g_2|^2}{\mu_1 P_{\text{TX}} |g_2|^2 + N_0}, \tag{14}$$

where P_{TX} and N_0 are the transmitted power of the UAV and noise power, respectively. Here, $|g_1|^2$ and $|g_2|^2$ are channel gains which can be calculated by substituting (3), (4), (5), (8), and (10) into (11), as

$$|g_1|^2 = \frac{1}{1 + A_{11} + A_{12} + \xi_{\text{NLoS}}}, \tag{15}$$

$$|g_2|^2 = \frac{1}{1 + A_{21} + A_{22} + \xi_{\text{NLoS}}}, \tag{16}$$

where A_{11}, A_{12}, A_{21}, and A_{22} are defined as follows:

$$A_{11} = \frac{\xi_{\text{LoS}} - \xi_{\text{NLoS}}}{1 + \alpha e^{-\beta\left(\frac{180}{\pi} \arctan\left(\frac{h}{R_1}\right) - \alpha\right)}}, \tag{17}$$

$$A_{12} = 20 \log_{10}\left(\frac{4\pi f_c}{c}\sqrt{R_1^2 + h^2}\right), \tag{18}$$

$$A_{21} = \frac{\xi_{\text{LoS}} - \xi_{\text{NLoS}}}{1 + \alpha e^{-\beta\left(\frac{180}{\pi} \arctan\left(\frac{h}{R_2}\right) - \alpha\right)}}, \tag{19}$$

$$A_{22} = 20 \log_{10}\left(\frac{4\pi f_c}{c}\sqrt{R_2^2 + h^2}\right). \tag{20}$$

Substituting (13)–(16) into (12), the packet transmission time T_i is computed as follows:

$$T_1 = \frac{\overline{B}}{\ln\left(1 + \frac{\mu_1 \gamma}{A_1}\right)}, \tag{21}$$

$$T_2 = \frac{\overline{B}}{\ln\left(1 + \frac{(1-\mu_1)\gamma}{\mu_1 \gamma + A_2}\right)}, \tag{22}$$

where $\gamma = \frac{P_{\text{TX}}}{N_0}$; A_1 and A_2 are defined as

$$A_1 = 1 + A_{11} + A_{12} + \xi_{\text{NLoS}}, \tag{23}$$

$$A_2 = 1 + A_{21} + A_{22} + \xi_{\text{NLoS}}. \tag{24}$$

We can see that A_1 and A_2 are always positive with $\forall\{h, R_1, R_2\}$.

IV. Optimization Algorithm For The UAV Altitude And User PAC

In this section, we propose an algorithm to determine the optimal values of the UAV altitude and the user PACs to achieve fairness among all users, making sure each user receive its packet from the UAV before the deadline set by the particular application. In other words, to make sure that no robot has a loss of connection, which may lead to unpredictable behavior, the UAV needs to adjust its system parameters such as height, transmitted power, etc., to guarantee reliable communication and fairness between the robots. Here, we consider the fairness condition as equal packet transmission time for all users and define it as $\delta T = |T_1 - T_2| = 0$. From (21) and (22), we have

$$\frac{\mu_1 \gamma}{A_1} = \frac{(1 - \mu_1)\gamma}{\mu_1 \gamma + A_2}, \tag{25}$$

which after few mathematical manipulations, can be rewritten as

$$\gamma \mu_1^2 + (A_2 + A_1)\mu_1 - A_1 = 0. \tag{26}$$

It is easy to see that this quadratic equation with variable μ_1 has $\Delta > 0$ and $-\gamma A_1 < 0$, $\forall\{\gamma, h, R_1, R_2\}$, i.e.,

$$\Delta = (A_2 + A_1)^2 + 4\gamma A_1 > 0, \tag{27}$$

$$\gamma(-A_1) = -\gamma A_1 < 0, \tag{28}$$

$$\mu_{1,2} = \frac{-(A_2 + A_1) \pm \sqrt{\Delta}}{2\gamma}. \tag{29}$$

Algorithm 1 Algorithm for determining μ_{1opt} and h_{opt}

Input: R_1, R_2 f_c, c, ξ_{LoS}, ξ_{NLoS}, α, β, γ, L, W, t_{out}.
Output: μ_{1opt}, h_{opt}.

function main
  Set the initial array: $h \leftarrow h_0{:}h_{max}$
  Set the initial index: $i_{idx} \leftarrow 0$
  for $i \leftarrow 1{:}\text{length}(h)$ **do**
    $\mu_1(i) \leftarrow \text{f}(h(i))$ ◁ (30)
    $T_{1i} \leftarrow \text{f}(h(i), \mu_1(i))$ ◁ (21)
    $T_{2i} \leftarrow \text{f}(h(i), \mu_1(i))$ ◁ (22)
    $|g_1|^2 \leftarrow \text{f}(h(i), R_1)$ ◁ (15)
    $|g_2|^2 \leftarrow \text{f}(h(i), R_2)$ ◁ (16)
    if Satisfy constraints in (31) **then**
      $i_{idx} \leftarrow i$;
      Break;
    end if
  end for
  return $\mu_1(i_{idx})$ and $h(i_{idx})$
end function

Hence, it has two roots, and the one with positive value is suitable for the PAC variable μ_1, given as

$$\mu_1 = \frac{-(A_2 + A_1) + \sqrt{\Delta}}{2\gamma}. \tag{30}$$

To achieve the fairness condition in the considered system, we need to find the values of h and μ_1 which satisfy the optimization problem as follows:

$$\begin{aligned} & \underset{h,\mu_1}{\delta T = 0} \\ \text{subject to} \quad & T_1 < t_{out}, \\ & T_2 < t_{out}, \\ & |g_1|^2 \geq |g_2|^2, \\ & \mu_1 < 0.5. \end{aligned} \tag{31}$$

In order to determine the optimal values of h and μ_1, **Algorithm 1** is executed following two steps.

- Step 1: Calculate the value of PAC μ_1 following the altitude of UAV h as in (30). Taking into account the height of buildings present in different environments, we select h_0 = 10 m as the minimum hight of UAV. In order to fly to a higher altitude and maintain the balance in there, the UAV needs more power. Thus, the smallest altitude of the UAV satisfying the other constraints is a good solution to address the power consumption problem of the UAV.
- Step 2: Check the constraints in (31) with a couple of values of μ_1 and h in step one. If these values of μ_1 and h satisfy (31), they are optimal values; if not, the altitude of UAV h increases and the algorithm returns to step one.

V. Numerical Results

In this section we present numerical results from the evaluation of the protocol considered above. The following system parameters are used: $W = 1$ MHz; $L = 4096$ bits; $f_c = 2$ GHz; $c = 3.10^8$ m/s; $t_{out} = 10$ ms; and other parameters are listed in Table I [15], [22].

Table I
SIMULATION PARAMETERS FOR STUDIED ENVIRONMENTS

Parameters	α	β	ξ_{LoS}	ξ_{NLoS}
Urban	9.61	0.16	1	20
Sub-urban	4.88	0.43	0.1	21
Dense-urban	12.08	0.11	1.6	23

First, we fix the simulation parameters to $R_1 = 80$ m, $R_2 = 150$ m, $h = 50$ m, $\gamma = 14$ dB, and find the optimal PAC of each user by applying **Algorithm 1**. It can be seen from the graph in Fig. 2 that an increase of PAC for U_1 leads to a reduction of the packet transmission time T_1 while the packet transmission time T_2 goes up. This is because T_1 is a decrease function following μ_1 whereas T_2 is the opposite to T_1. Further, we can see a couple of optimal values of $h = 50$ m and $\mu_1 = 0.3364$ that satisfy the fairness condition. Similarly, the optimal values of PAC for U_1 can be found for sub-urban and dense urban environments, and are equal to 0.3580 and 0.3747, respectively. The PAC for U_1 in the dense urban environment is the highest because all users experience also the strongest NLoS here.

Next, we consider the effect of changing the transmission power of the UAV, γ, using the optimal altitude and the optimal PAC for each user with $R_1 = 80$ m, $R_2 = 150$ m, Fig. 3-4. From Fig. 3, we make the following observations: First, the solid line shows that when the height of the UAV decreases to the minimum altitude of $h_0 = 10$ m, the transmitted power should be increased to overcome the effects of higher probability of strong NLoS. Second, comparing the three considered types of environments, we can see that the dense urban environment requires the most power due to the presence of multiple obstacles and thus higher chances of NLoS.

Furthermore, the results in Fig. 4 show that: Firstly, when the transmitting power of the UAV increases, the factor μ_1 also raises slightly until the altitude of UAV reaches the smallest value of $h_0 = 10$ m. This is due to the increasing probability of the user to experience strong NLoS. Secondly, when the height of UAV does not change following the increasing γ, the PAC for U_1 decreases because U_2 needs more power to decode its signal.

Fig. 5-6 show the optimal height of the UAV and the optimal PAC for U_1 as functions of varying distance between U_2 and the UAV (R_1 is fixed to 80 m, γ = 14.6 dB). It can be seen from Fig. 5 that when the distance between the UAV and U_2 grows, the optimal altitude of UAV increases in all three different environments. This can be explained by the fact that the increasing distance between the UAV and U_2 results in an increasing height of the UAV needed to obtain a coverage region including U_2 and to reduce the probability of the user to experience strong NLoS. Similar to the results in Fig. 3, Fig. 5 shows that the altitude of the

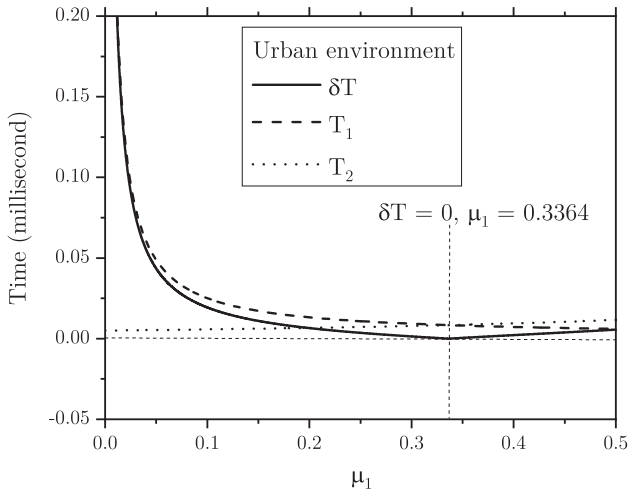

Figure 2. T_1, T_2, δT in the urban environment.

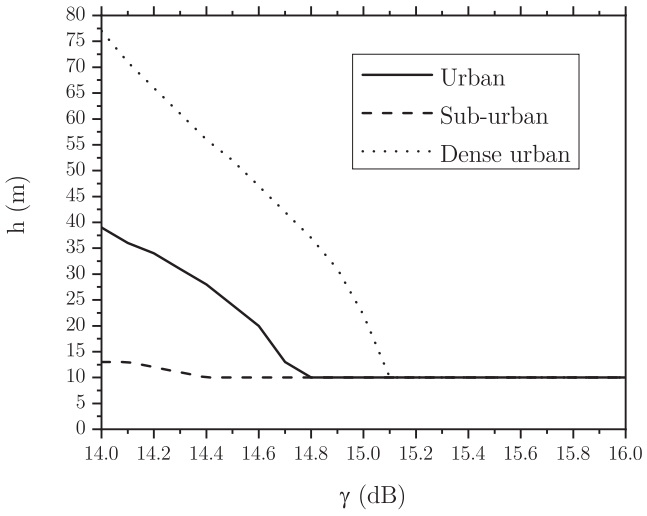

Figure 3. The effect of P_{TX} on the optimal value of h.

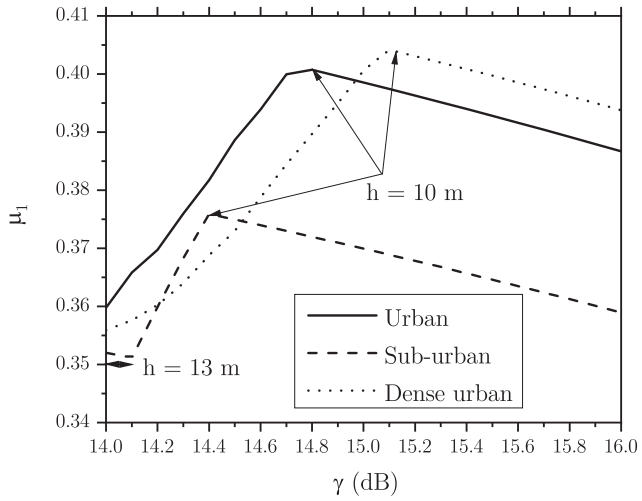

Figure 4. The effect of P_{TX} on the optimal value of μ_1.

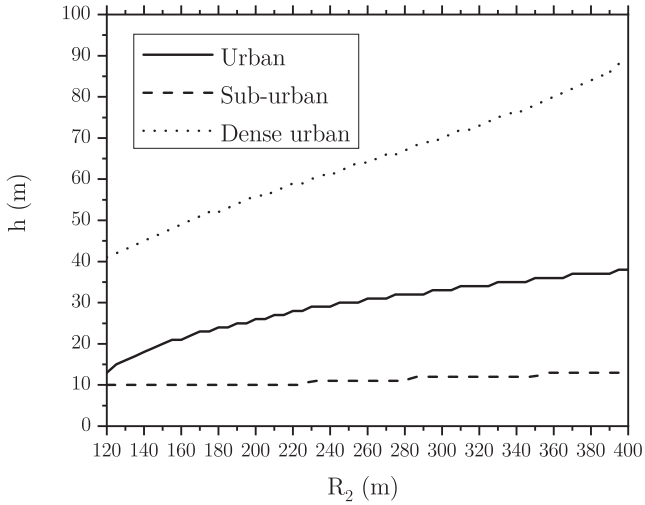

Figure 5. The effect of R_2 on the optimal value of h.

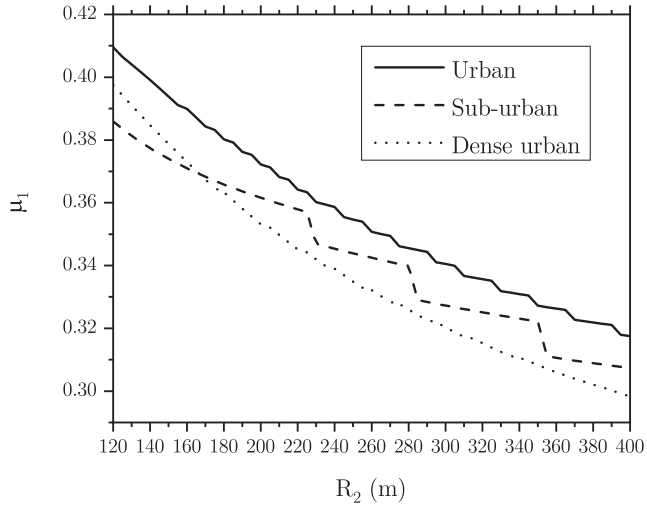

Figure 6. The effect of R_2 on the optimal value of μ_1.

UAV in dense urban environment is the highest, while that in sub-urban is the lowest. In addition, we can observe from Fig. 6 that μ_1 decreases when U_2 moves further away from the UAV as in this case U_2 needs more power in order to deal with the increasing probability of the user experiencing strong NLoS. In addition, the PAC for U_1 declines slower in rural environment compared with the other environments due to the smaller chances of strong NLoS in sub-urban environments. This is also the reason why the height of the UAV changes slightly as shown in Fig. 5.

We also look at how the length of the packet and the UAV's transmitting power affect the optimal height of the UAV and the optimal PAC for U_1 satisfying the fairness condition in urban environment with $R_1 = 80$ m, $R_2 = 200$ m. It can be seen from Fig. 7 that when the size of the packet increases, the altitude of the UAV also grows (while the power allocation coefficient for U_1 decreases, Fig. 8). This is because an increase in the size of the packet leads

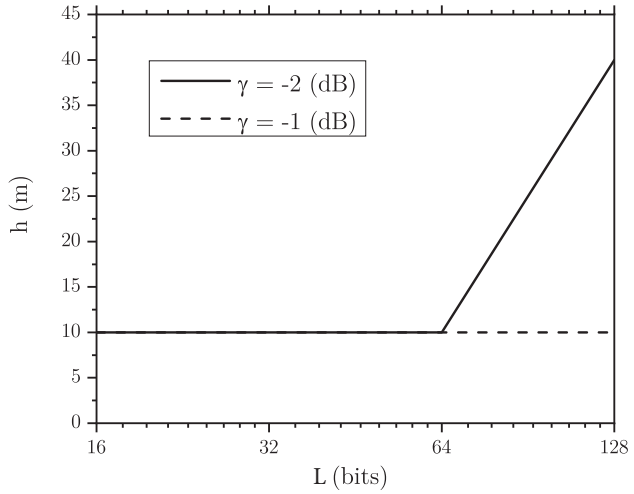

Figure 7. The effect of L on the optimal value of h.

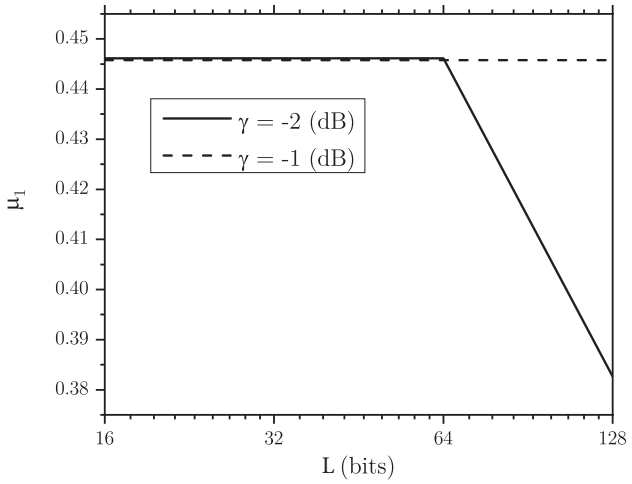

Figure 8. The effect of L on the optimal value of μ_1.

to larger packet transmission time, which might result in varying channel characteristics during the transmission time of one packet. In addition, when the transmitting power of the UAV increases, it can deal with an increasing NLoS, thus, the values of h and μ_1 do not change for the case of γ = 1 dB.

VI. Conclusions And Future Work

In this work we investigated a UAV assisted wireless communication system using NOMA and proposed an algorithm for finding the optimal values of the altitude of the UAV and the PAC for each user. We looked at the dependencies between the fairness among users and the UAV altitude and PAC for all users, and found the optimal values of the altitude of the UAV and the users' PAC given different types of communication environments. It can be concluded that UAV assisted communications has many benefits, especially for ad hoc communications in time sensitive applications with high reliability requirements. In the future work, we will consider a scenario with a larger amount of communicating devices, account for node mobility and multi-path fading.

Acknowledgments

This work was partially supported by the European Commission under the project FORA with grant number 764785, and Swedish Foundation for Strategic research via the project FiC.

References

[1] M. Mozaffari, W. Saad, M. Bennis, Y.-H. Nam, M. Debbah, "A tutorial on UAVs for wireless networks:applications, challenges, and open problems," *arXiv:1803.00680 [cs.IT]*, Mar. 2018.

[2] M. Erdelj, E. Natalizio, K. R. Chowdhury, and I. F. Akyildiz, "Help from the sky: Leveraging UAVs for disaster management," *IEEE Pervasive Comput.*, vol. 16, no. 1, pp. 24–32, Jan. 2017.

[3] A. Merwaday, A. Tuncer, A. Kumbhar, and I. Guvenc, "Improved throughput coverage in natural disasters: Unmanned aerial base stations for public-safety communications," *IEEE Veh. Tech. Mag.*, vol. 11, no. 4, pp. 53–60, Dec. 2016.

[4] Y. Zeng, R. Zhang, and T. J. Lim, "Wireless communications with unmanned aerial vehicles: opportunities and challenges," *IEEE Commun. Mag.*, vol. 54, no. 5, pp. 36–42, May 2016.

[5] Z. Ding, X. Lei, G. K. Karagiannidis, R. Schober, J. Yuan, and V. K. Bhargava, "A survey on non-orthogonal multiple access for 5G networks: Research challenges and future trends," *IEEE JSAC*, vol. 35, no. 10, pp. 2181–2195, Oct. 2017.

[6] P. K. Sharma and D. I. Kim, "UAV-enabled downlink wireless system with non-orthogonal multiple access," in *Proc. IEEE GLOBECOM Workshops*, Dec. 2017, pp. 1–6.

[7] M. F. Sohail, C. Y. Leow, and S. Won, "Non-orthogonal multiple access for unmanned aerial vehicle assisted communication," *IEEE Access*, vol. 6, pp. 22 716–22 727, 2018.

[8] M. Mozaffari, W. Saad, M. Bennis, and M. Debbah, "Drone small cells in the clouds: Design, deployment and performance analysis," in *Proc. IEEE GLOBECOM*, San Diego, CA, USA, Dec. 2015, pp. 1–6.

[9] Y. Chen, W. Feng, and G. Zheng, "Optimum placement of UAV as relays," *IEEE Commun. Lett.*, vol. 22, no. 2, pp. 248–251, Feb. 2018.

[10] M. Gruber, "Role of altitude when exploring optimal placement of UAV access points," in *Proc. IEEE WCNC*, Doha, Qatar, Apr. 2016, pp. 1–5.

[11] K. Higuchi and A. Benjebbour, "Non-orthogonal multiple access (NOMA) with successive interference cancellation for future radio access," *IEICE Trans.*, vol. 98-B, pp. 403–414, 2015.

[12] Y. Saito, Y. Kishiyama, A. Benjebbour, T. Nakamura, A. Li, and K. Higuchi, "Non-orthogonal multiple access (NOMA) for cellular future radio access," in *Proc. IEEE VTC*, Dresden, Germany, Jun. 2013, pp. 1–5.

[13] L. Dai, B. Wang, Z. Ding, Z. Wang, S. Chen, and L. Hanzo, "A survey of non-orthogonal multiple access for 5G," *IEEE Commun. Surveys Tuts.*, vol. 20, no. 3, pp. 2294–2323, Thirdquarter 2018.

[14] Q. Feng, J. McGeehan, E. K. Tameh, and A. R. Nix, "Path loss models for air-to-ground radio channels in urban environments," in *Proc. IEEE VTC*, vol. 6, May 2006, pp. 2901–2905.

[15] R. I. Bor-Yaliniz, A. El-Keyi, and H. Yanikomeroglu, "Efficient 3-D placement of an aerial base station in next generation cellular networks," in *Proc. IEEE ICC*, Kuala Lumpur, Malaysia, May 2016, pp. 1–5.

[16] M. Mozaffari, W. Saad, M. Bennis, and M. Debbah, "Unmanned aerial vehicle with underlaid device-to-device communications: Performance and tradeoffs," *IEEE Trans. Wireless Commun.*, vol. 15, no. 6, pp. 3949–3963, Jun. 2016.

[17] Z. Ding, Z. Yang, P. Fan, and H. V. Poor, "On the performance of non-orthogonal multiple access in 5G systems with randomly deployed users," *IEEE Signal Process. Lett.*, vol. 21, no. 12, pp. 1501–1505, Dec. 2014.

[18] N. B. Mehta, V. Sharma, and G. Bansal, "Performance analysis of a cooperative system with rateless codes and buffered relays," *IEEE Trans. Wireless Commun.*, vol. 10, no. 4, pp. 1069–1081, Apr. 2011.

[19] T. M. C. Chu, H. Phan, and H. Zepernick, "On the performance of underlay cognitive radio networks using M/G/1/K queueing model," *IEEE Commun. Lett.*, vol. 17, no. 5, pp. 876–879, May 2013.

[20] H. Tran, T. Q. Duong, and H. Zepernick, "Performance of a spectrum sharing system over Nakagami-m fading channels," in *Proc. IEEE ICSPCS*, Gold Coast, QLD, Australia, Dec. 2010, pp. 1–6.

[21] F. A. Khan, K. Tourki, M. Alouini, and K. A. Qaraqe, "Delay performance of a broadcast spectrum sharing network in Nakagami-m fading," *IEEE Trans. Veh. Technol.*, vol. 63, no. 3, pp. 1350–1364, Mar. 2014.

[22] A. Al-Hourani, S. Kandeepan, and A. Jamalipour, "Modeling air-to-ground path loss for low altitude platforms in urban environments," in *Proc. IEEE GLOBECOM*, Austin, TX, USA, Dec. 2014, pp. 2898–2904.